Stochastic Modeling of Filtration with Sieving in Graded Pore Networks

Binan Gu[1], Pejman Sanaei[2], Lou Kondic[3], Linda J. Cummings[3]

[1]Department of Mathematical Sciences, Worcester Polytechnic Institute, Worcester, MA 01609, USA
[2]Department of Mathematics and Statistics, Georgia State University, Atlanta, GA 30302, USA
[3]Department of Mathematical Sciences, New Jersey Institute of Technology, Newark, NJ 07102-1982, USA

1. Introduction

Membrane filtration of fluids is ubiquitous in daily life and commercial practice. There is increasing interest from industrial practitioners in mathematical models that capture the complex nature of the process. We focus on filtration through membranes whose internal structure is a network of pores (see Fig. 1) through which foulant-laden fluid flows, with two modes of membrane fouling operating simultaneously - adsorption and sieving. Adsorption involves a slow accretion of foulant particles far smaller than pore sizes on the pore wall, while sieving concerns much larger particles that block pore entrances on a faster time scale. We model adsorption as a diffusive-convective continuum transport process, and sieving as a stochastic (Poisson) process on the network with a simulation-based approach. We investigate how the two fouling mechanisms interact and affect performance measures such as filter lifetime and flux evolution.

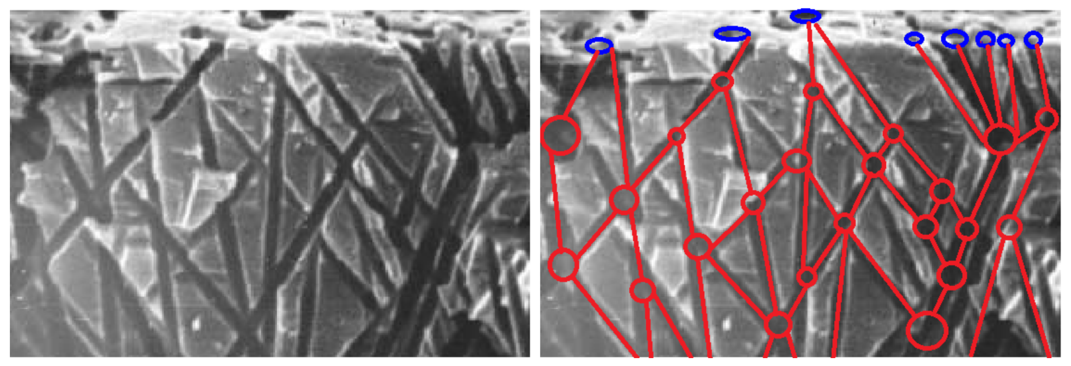

Figure 1: (left) an experimental image with lateral view of a filter cross-section [6]; (right) a corresponding (partial) graph representation with inlets on the top surface (blue) and interior pore junctions and throats (red).

In the network representation, pore throats are modeled as cylindrical tubes of specified initial radii (the edges), connected at pore junctions (the nodes). The edges shrink over time due to small contaminant particles clogging the pore space (adsorption), and can be instantly blocked by larger particles (sieving). We aim to answer the following questions of practical concern:

1. Is there a critical Poisson arrival rate separating adsorption-dominated and sieving-dominated regimes?
2. If so, how does this threshold depend on foulant particle size and pore-size gradient across the filter?
3. How do pore-size gradients and the arrival rate of sieving particles affect the foulant distribution in the filter?

2. Pore Network Construction

We consider membrane filters of uniform porosity, but with a negative pore-size gradient in the depth of the filter (larger pores upstream). We generate representative artificial filter pore networks by distributing vertices randomly within a square prism of cross-sectional length W and height $2W$ (2D schematic in Fig. 2, left). The prism is divided into 4 central bands as indicated; to maintain fixed porosity and a specified pore-size gradient the number of vertices within each band must vary. We enforce maximum and minimum pore lengths, $WD_{\max}, WD_{\min}$, and connect all vertices whose separation lies between these two values by cylindrical pores (a minimum pore radius is needed to justify a Hagen-Poiseuille model for fluid dynamics through the pore network). Periodic connections are enforced across opposite walls of the prism, indicated by the dash-dotted lines.

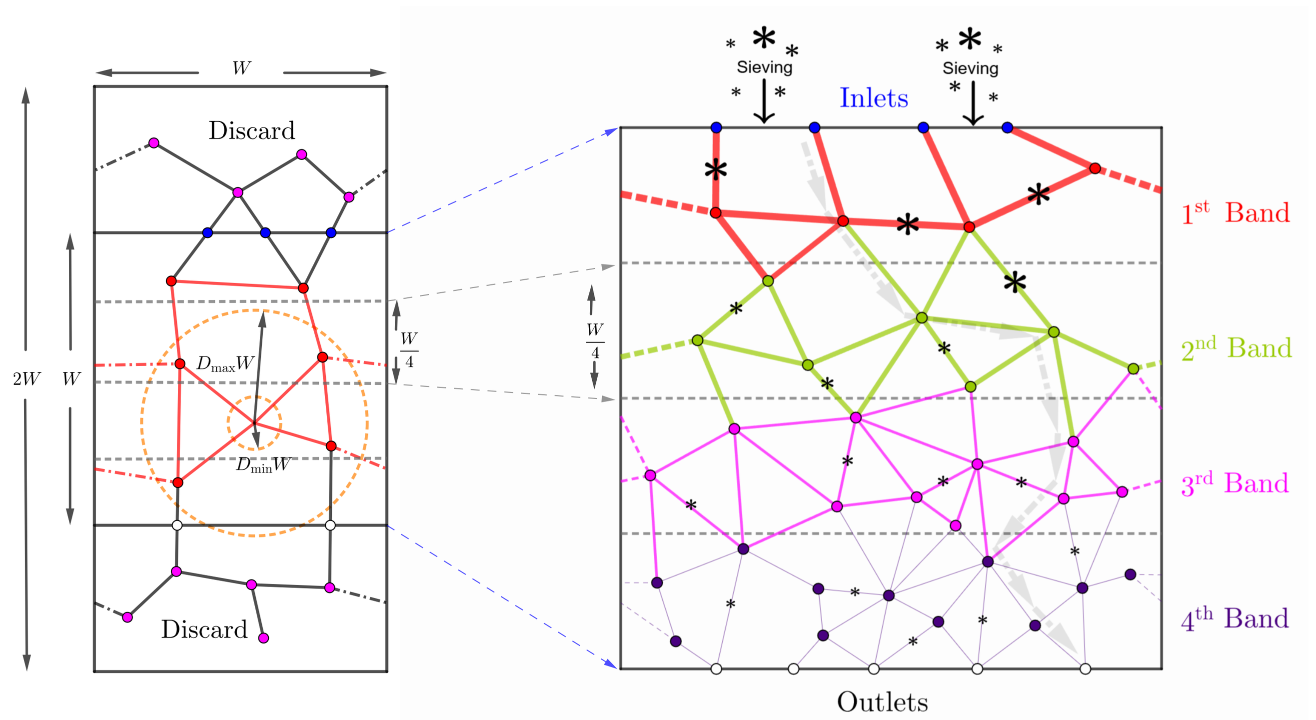

Figure 2: Left panel: red filled circles are interior vertices, V_{int}, blue filled circles are induced inlets V_{in}, and white filled circles are induced outlets V_{out}. Black solid horizontal lines are cutting lines (planes in 3D), and magenta circles are discarded points. orange dotted circles form the search annulus enforced by $D_{\max}$ and $D_{\min}$. Right panel: After cutting. Colored junctions and pores distinguish the different bands. Black stars denote sieving particles; light gray arrows show possible transit paths through the network.

To generate inlets and outlets, we cut the prism to isolate a central cube of side length W. The resulting network, schematized in 2D in Fig. 2 at right, has 4 equal size bands of fixed porosity, with a constant pore-size gradient from one band to the next. Pores in the kth band have radius r_k.

$$r_k = r_m + (m-k)\,s, \qquad 1 \le k \le m, \tag{1}$$

where s is the pore radius gradient, m is the number of bands (here $m=4$) and r_m is the pore radius in the bottom band. Actual networks are 3D and have thousands of pores.

3. Mathematical Model

We model filtration of a feed solution, assumed Newtonian with viscosity μ, containing a continuum concentration C_0 of small foulant particles that are transported through the pore network via diffusion and adsorption and deposited on pore walls; and much larger sieving particles (comparable to the pore radius) that can catastrophically block pores. Filtration is driven by a fixed pressure difference P_0 across the membrane. We scale all lengths with membrane thickness W, pressure with P_0, fluid flux with $\pi W^3 P_0/(8\mu)$ and time with the adsorptive fouling timescale, $W/(\Lambda\alpha C_0)$.

Here, Λ is an adsorption coefficient with dimensions length/time representing the affinity of the adsorptive fouling particles for the membrane; α is the volume occupied by such a particle when deposited on the pore wall.

Flow through pore network: Fluid flow through the network is modelled by Hagen-Poiseuille (H-P) equations. Under the above scalings and assumptions, volumetric flux q_{ij} through each pore e_{ij} connecting vertices v_i and v_j is governed by

$$q_{ij}(t) = k_{ij}(t)\left(p_i(t) - p_j(t)\right), \tag{2}$$

where $p_i(t)$ is the pressure at vertex i at time t and $k_{ij}(t)$ is the conductance of the pore,

$$k_{ij}(t) = \frac{1}{\int_0^{\ell_{ij}} \frac{1}{r_{ij}^4(y,t)}\,dy} \tag{3}$$

determined by the instantaneous pore geometry (length ℓ_{ij} and radius $r_{ij}(y,t)$, where local axial coordinate y is measured along the pore). Conservation of mass at pore junctions yields a network-scale problem for the pressure at each vertex, which is readily solved using a graph Laplacian formulation. We then determine the distribution of fluxes throughout the pore network.

Adsorptive Fouling: Adsorptive particle transport is governed by diffusion and advection. An asymptotic analysis based on the (typically large) axial Peclet number suggests that diffusion dominates transport in the radial direction (giving a particle concentration that is radially uniform), while advection dominates in the axial direction, leading to a system of simple 1D advection equations for particle concentration $c_{ij}(y,t)$ along each pore axis. This can be solved in terms of the local pore radius $r_{ij}(y,t)$, and coupled to the evolution equation for $r_{ij}(y,t)$, which shrinks in response to the local concentration $c_{ij}(y,t)$. Again, the final system can be efficiently solved via the graph Laplacian for the foulant concentration $c_i(t)$ at vertex v_i.

Sieving: Sieving particles are assumed to arrive at the membrane top surface following a Poisson process $n(t)$ with rate (per edge) γ, i.e. the probability of k such particles having arrived by time t is

$$\text{Prob}\,(n(t) = k) = \frac{(\gamma t)^k}{k!}e^{-\gamma t}, \quad k = 0,1,2,\dots. \tag{4}$$

We consider monodisperse spherical particles of specified size for each Poisson simulation, but can extend to general particle size distributions. We make the following assumptions:

1. When a particle arrives at an inlet it performs a random walk through the pore network with transition probabilities determined according to preferential flow (below). During this random walk, adsorption is suspended (due to timescale differences) until the sieving particle escapes or blocks a pore.
2. An edge is completely blocked when a particle traveling according to preferential flow enters a pore whose radius is smaller than the particle's. Blocking is irreversible.

Preferential flow: The probability that a sieving particle arrives at a given inlet $v_i \in V_{\text{in}}$ is quantified by the proportion of outgoing flux at that inlet relative to the total outgoing flux from all inlets. After the walker chooses an inlet it traverses the network following *preferential flow*: The probability of moving from v_i to v_j (via a direct edge connection e_{ij}) is defined by the transition probability $\mathcal{P}_{ij}(t)$:

$$\mathcal{P}_{ij}(t) := \begin{cases} \dfrac{q_{ij}(t)}{\sum_{v_j\in\mathcal{N}_i} q_{ij}(t)}, & \forall v_i \in V\backslash V_{\text{out}} \quad \text{(flux-weighted random walk)}; \\ \delta_{ij}, & \forall v_i \in V_{\text{out}} \quad \text{(absorbing at bottom surface)}, \end{cases} \tag{5}$$

where $\mathcal{N}_i$ is the set of neighbors of v_i, V is the set of all vertices, V_{out} is the set of outlet vertices, and δ_{ij} is the Kronecker delta.

4. Performance Measures

To make quantitative comparisons between different membrane filters we introduce two key performance measures: throughput $h(t)$, the volume of filtrate captured up to the specified time t; and accumulated foulant concentration $c_{\text{acm}}(t)$, the (adsorptive) foulant concentration in the cumulative collected filtrate at time t.

5. Results

We simulate the above system on representative large pore networks with a focus on the effect of the sieving particle arrival rate γ, the sieving particle size p_{size}, and the pore-size gradient s (see Eq. (1) and the table below). To obtain good statistical averages we carry out 120 simulations for each γ-value. Simulations are run to time t_{final} at which flux through the filter falls to zero.

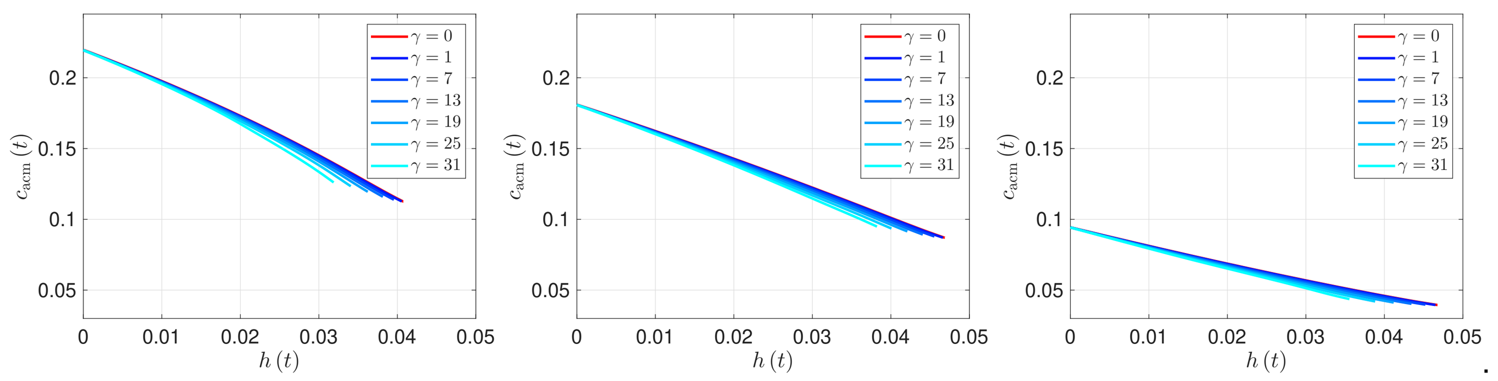

Figure 3: Accumulated foulant concentration at membrane outlet vs throughput for networks with pore radius gradient $s=0$ (left; ungraded), $s=0.0015$ (center; moderate gradient) and $s=0.003$ (right; strongly-graded).

Initial Radius	$s=0$ (Ungraded)	$s=0.0015$ (Moderate)	$s=0.003$ (Strong)
Band 1	0.01	0.01225	0.0145
Band 2	0.01	0.01075	0.0115
Band 3	0.01	0.00925	0.0085
Band 4	0.01	0.00775	0.0055

Figure 3 shows results for three different values of the pore size gradient, s, for sieving particle size $p_{\text{size}} = 0.0078$. These results indicate that a filter with a pore-size gradient gives better results than one with uniform pore sizes, across a range of sieving particle arrival rates (the case $\gamma = 0$ corresponds to sieving only). In particular, the filter with the strongest pore size gradient performs best overall, with less accumulated foulant than other cases, and comparable throughput to the moderately-graded filter.

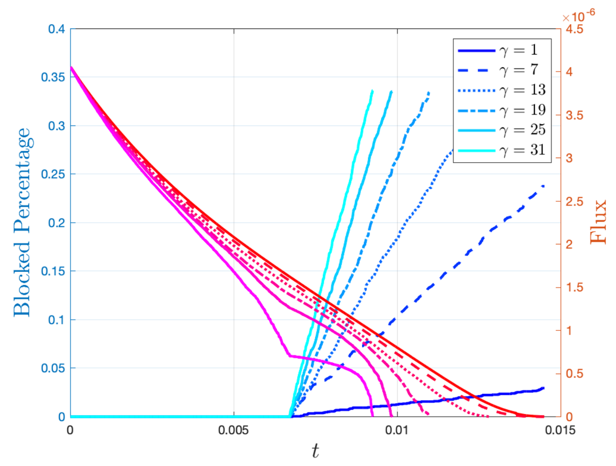

(a) Band 1

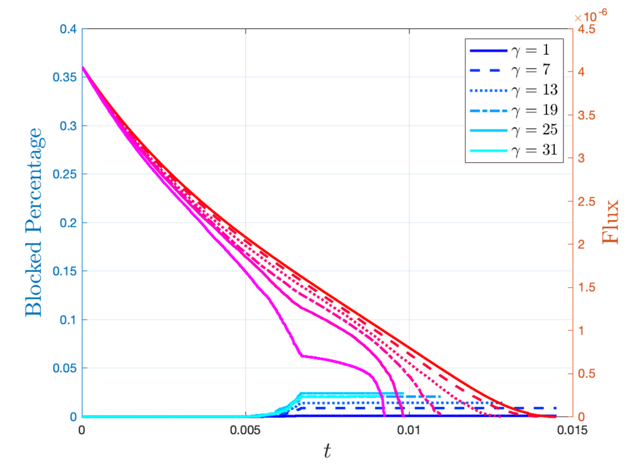

(b) Band 2

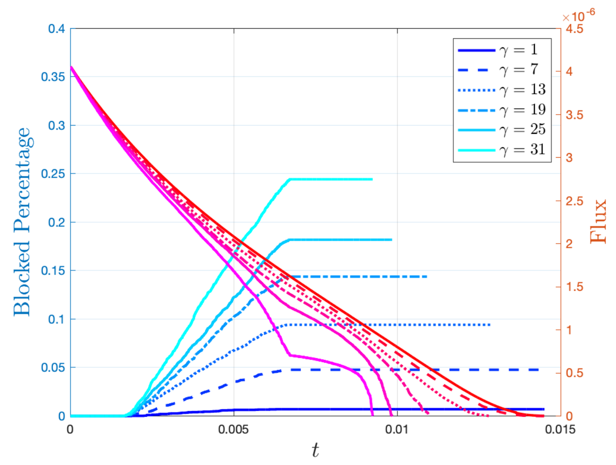

(c) Band 3

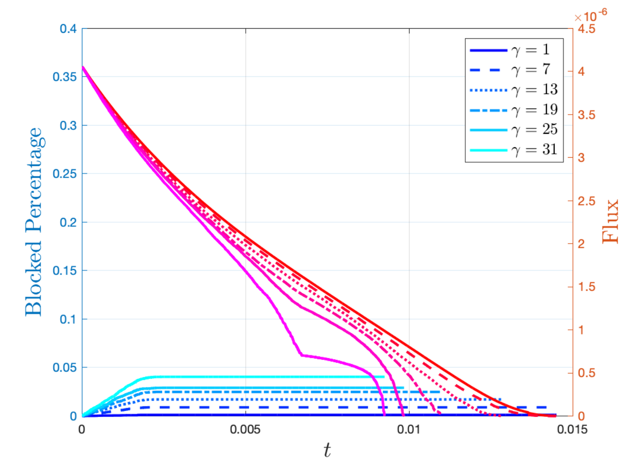

(d) Band 4

Figure 4: Blocked pore fraction and flux against time, for bands 1-4 (strongly-graded filter).

To further probe the strongly-graded system we plot in Fig. 4 the fraction of pores blocked by a sieving particle (blue curves) over time in each band of the filter, alongside the flux (red/pink curves). Sieving particles are small enough to initially pass through the first three layers but not the fourth. Note the sequential nature of the sieving: first band 4 exhibits blocking, then band 3, then band 2 and finally band 1. At large γ the onset of blocking in band 1 is accompanied by a strong change of curvature in the flux curves.

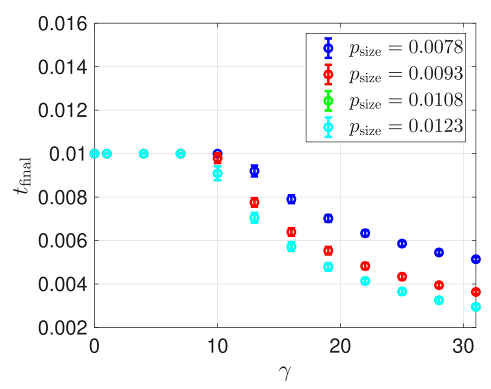

(a) Ungraded filter

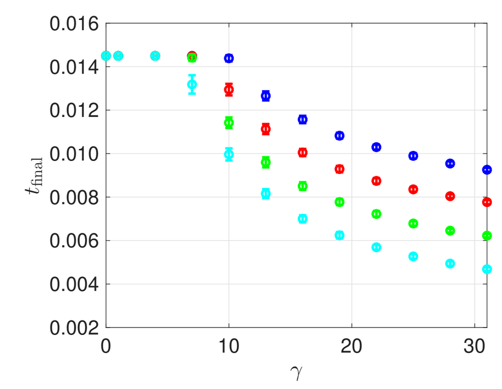

(b) Large pore-size gradient

Figure 5: Filter lifetime vs sieving particle arrival rate, exhibiting bifurcation.

Fig. 5 shows how filter lifetime changes as the sieving particle arrival rate γ is increased, for filters with uniform pores and with a large pore-size gradient. When γ is small, all sieving particle sizes yield the same filter lifetime for a given pore-size gradient (overlapped colors), indicating that adsorptive fouling alone determines lifetime. As γ increases, a bifurcation is observed, beyond which sieving strongly influences lifetime. The bifurcation occurs at the same γ-value for all p_{size} for the ungraded filter, but depends on p_{size} for the graded filter. In all cases, for sufficiently high γ the lifetime is shorter for larger sieving particles.

6. Conclusions and Future Work

We have formulated a pore network model of a membrane filter that can simulate adsorptive and sieving fouling regimes simultaneously. Our model can account for pore-size gradients in the filter, and shows that such gradients can improve performance. The model simulations also exhibit a phase transition in filter lifetime as the frequency of sieving events increases, that depends on particle size and pore-size gradient.

Future work will focus on developing a mean-field probabilistic approach to the stochastic sieving problem, which will obviate the need for running many Poisson simulations and make it feasible to investigate simultaneously the effect of pore network variations (current simulations for each pore-size gradient are run on a single representative network).

7. Acknowledgements

We thank NSF for their funding of this project: NSF DMS-1615719, NSF DMS-2201627.

References

[1] Gu, B., Renaud, D. R., Sanaei, P., Kondic, L. and Cummings, L. J., " On the Influence of Pore Connectivity on Performance of Membrane Filters ", *J. Fluid Mech.*, 2020, vol. 902, pp. A5.

[2] Gu, B., Kondic, L. and Cummings, L. J., "A Graphical Representation of Membrane Filtration", *SIAM Journal of Applied Mathematics*, 2022, vol. 82, pp. 950-975.

[3] Gu, B., Kondic, L. and Cummings, L. J., "Flow through Pore-Size Graded Membrane Pore Networks", *Physical Review Fluids*, 2023, vol. 8, pp. 044502.

[4] Gu, B., Kondic, L. and Cummings, L. J., "Network-based membrane filters: Influence of network and pore size variability on filtration performance", *Journal of Membrane Science*, 2022, vol 657, pp. 120668.

[5] Gu, B., Sanaei, P., Kondic, L. and Cummings, L. J., "Stochastic Modeling of Filtration with Sieving in Graded Pore Networks", *Under revision at J. Fluid Mech.*.

[6] Apel, P., "Track etching technique in membrane technology", *Radiation Measurements*, 2001, vol 34, pp. 559-566.